International Communications in Heat and Mass Transfer 43 (2013) 57–62

Contents lists available at SciVerse ScienceDirect

International Communications in Heat and Mass Transfer

journal homepage: www.elsevier.com/locate/ichmt

Effect of non-uniform heating on the performance of the microchannel heat sinks ☆

Chun-Kai Liu [a], Shu-Jung Yang [a], Yu-Lin Chao [a], Kun Ying Liou [b], Chi-Chuan Wang [b,*]

[a] Electronics and Optoelectronics Research Laboratories, Industrial Technology Research Institute, Hsinchu 310, Taiwan
[b] Department of Mechanical Engineering, National Chiao Tung University, Hsinchu 300, Taiwan

ARTICLE INFO

Available online 5 March 2013

Keywords:
Microchannel
Non-uniform heating
Heat sink

ABSTRACT

The present study experimentally investigates the performance of a 2-pass microchannel heat sink subject to non-uniform heating. The size of the microchannel heat sink is 132 mm×82 mm×6 mm with a rectangular channel of 1 mm×1 mm. Three independent heaters having identical size (96 mm×38.5 mm×1 mm) is placed consecutively below the microchannel heat sink. Two kinds of manifolds are used for testing of the microchannel, one with a side entrance (type A) and the other with a front entrance (type B). Test results show that both maximum temperature and average temperature rise with the total input power, and this is applicable for both manifolds. For uniform heating condition, the maximum temperature for type B manifold is much lower than that for type A manifold due to a better flow distribution and heat transfer performance. The pressure drop is slightly reduced with the rise of supplied power. For non-uniform heating, the maximum temperature and the average temperature depend on the location of heaters. For the same supplied power with non-uniform heating, it is found that heater being placed at the inlet of the microchannel will give rise to a higher maximum temperature than that being placed at the rear of the heat sink. This phenomenon is especially pronounced when the inlet flowrate is comparatively small and becomes less noted as the inlet flowrate is increased to 0.7 L/min.

1. Introduction

The microelectronic industry has continued to follow the Moore's law of increasing transistor density on a single chip [1]. Hence, the heat dissipation density of a typical chip has risen dramatically since more and more transistors are being packed in a confined area. As a consequence, thermal management exploiting conventional air-cooling becomes insufficient to handle the increasing heat dissipation of the current and future microprocessors. In this regard, single phase liquid cooling for microprocessors has been recognized as an effective alternative for the high flux applications. Liquid cooling employing microchannel design is especially promising for it provides effective heat removal within a limited space. However, there are two major issues in association with liquid-cooled microchannel heat sink. The first is the liquid flow distribution alongside the multiple microchannels and the second problem is inherited with the nature of electronic devices whose heat source is normally non-uniform. The presence of non-uniform heating may substantially raise the temperature for its gigantic spreading resistance.

In recent years, there had been some studies concerning the influence of inlet location on the flow distribution of a liquid-cooled heat sink. For example, Lu and Wang [2] studied five different inlet locations, namely I-type, Z-type,]-type, L-type and Γ-type, on the overall performance of a multiple liquid-cooled heat sink. Their results showed that the heat transfer performance for I-type outperforms other inlet arrangements. Ljubisa et al. [3] designed a microchannel having a splitting flow arrangement which can considerably reduce the pressure drop of the microchannel heat sink.

Since both heat transfer and pressure drop must be considered in optimizing the performance of the microchannel heat sinks. Toh et al. [3] performed a 3-D numerical simulation of the microchannels, and they reported that at lower Reynolds number the temperature of the water increases, leading to a decrease in the viscosity and hence smaller frictional losses. Park et al. [4] numerically examined the effect of rectangular channel size on the performance of microchannels. They found that there were deviations between the experimental and theoretical values of the heat transfer rate in the microchannels, and they proposed an empirical correlation to amend the deviations. Liu et al. [5] use a PIV technique to measure velocity distribution of microchannel subject to five different inlet arrangements, and their measured results are generally in line with the numerical calculation by Lu and Wang [2].

The foregoing results are mainly associated with uniform heating condition. In practical application, the surface heat flux may not be uniform, and this is commonly encountered in typical IGBT/diode high power module. However, relevant researches on this topic are very rare. Lelea [6] numerically investigated the effect of partially heated perimeter on the microchannel. He found that the partial heating together with variable viscosity casted a strong influence on the thermal and hydrodynamic characteristics of the micro-heat

☆ Communicated by W.J. Minkowycz.

* Corresponding author at: EE474, 1001 University Road, Hsinchu 300, Taiwan.
E-mail address: ccwang@mail.nctu.edu.tw (C.-C. Wang).

0735-1933/$ – see front matter © 2013 Elsevier Ltd. All rights reserved.
http://dx.doi.org/10.1016/j.icheatmasstransfer.2013.02.003

Nomenclature

D_h	hydraulic diameter, mm
P	supplied power into the heater, W
Pr	Prandtl number, dimensionless
Q	heat transfer rate carried by water coolant, W
Q_{avg}	average heat transfer rate, $Q_{avg} = \frac{Q_{sup}+Q}{2}$, W
Q_{losg}	heat loss through the bakelite, W
Q_{sup}	supplied input to the microchannel heat sink, W
Re	Reynolds number, dimensionless
T	temperature, °C
T_{in}	water inlet temperature, °C
T_{out}	water outlet temperature, °C
x	axial coordinate from the entrance of the microchannel, m
x^+	dimensionless axial coordinate, $x^+_{\text{fully devloped}} = \frac{x}{D_h \text{RePr}}$

sink. Cho et al. [7,8] investigated the cooling performance of the microchannel heat sinks under various heat flux conditions subject to different geometry and header locations. Thermal load is applied to the microchannel heat sinks by nine separate heaters in order to provide a uniform or non-uniform heat flux. Their results indicated that the straight microchannels are less sensitive to the temperature distributions.

As seen, very few researches were concerned with the influence of non-uniform heating on the performance of the microchannel heat sink, yet the experimental data is especially rare. In this regard, it is the objective of this study to provide some experimental data on this subject.

2. Experimental setup

The schematic of the experimental apparatus is depicted in Fig. 1. The test rig is composed of a water cooling loop, a data acquisition system, and a water thermostat. The water thermostat is to maintain a fixed inlet water temperature into the test section. The water loop consists of a centrifugal pump (Iwaki Corp., model MD-20RZ) which delivers water coolant alongside the piping and into the test section. The water pump can provide a volumetric flowrate from 0.1 to 1 L/min. A pre-calibrated rotameter is installed between the water pump and the test section. The uncertainty of the volumetric flowrate is less than 0.005 L/min of the test span. The test sample is a two-pass microchannel heat sink with two different designs of manifold. The manifolds are characterized as long edge (type A) or short edge (type B). The long edge manifold denotes a side inlet entrance which is normal to the main flow direction while the inlet of the short edge manifold is parallel to the flow direction. The size of type A manifold is 10 mm × 102 mm × 21 mm. The size of inlet and outlet manifolds is identical. The size of the type B manifold is 25 mm × 90 mm × 14 mm. Schematic of the flow direction in and out the microchannel for type A and type B manifolds is schematically shown in Fig. 2. The size of the microchannel heat sink is 132 mm × 82 mm × 6 mm and is made of cooper. The rectangular

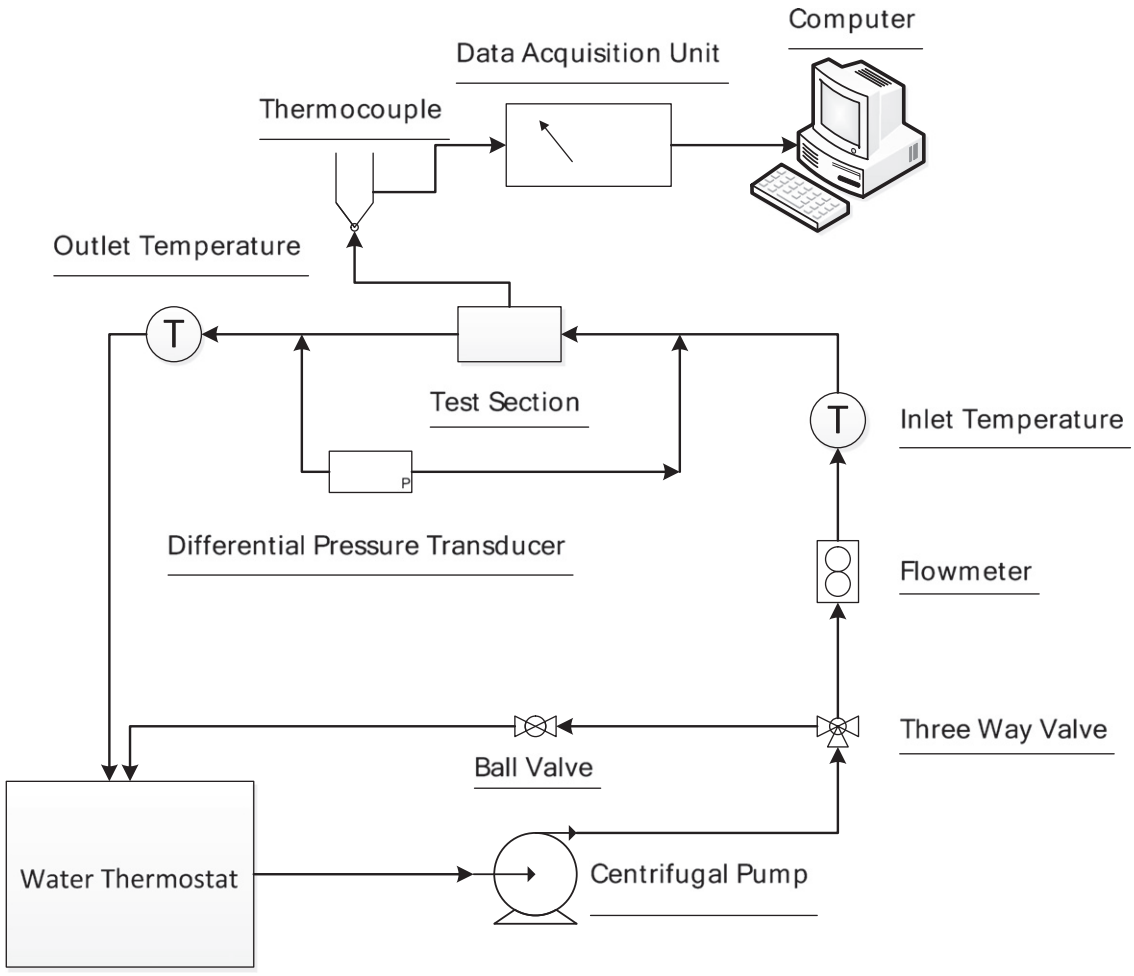

Fig. 1. Schematic of the test setup.

channel size is 1 mm × 1 mm, and each pass has a total of fifteen channels. The channel is located in the middle of the copper plate, indicating a wall thickness of 2.5 mm for the microchannel heat sink.

A differential pressure transducer (Yokogawa, model EJA110-DM) is used to measure the pressure drop across the test section with an accuracy of 0.1% of the test span. The inlet and outlet water temperatures were measured by two precision RTDs with calibrated accuracies of 0.1 °C. A total of six T-type thermocouples are used to measure the surface temperature beneath the cold plate. The locations of the thermocouples are shown in Fig. 3(a). Notice that the thermocouples were pre-calibrated from 20 °C to 80 °C, with a calibrated accuracy of 0.1 °C. All the measured temperatures were recorded by a data acquisition unit (Yokogawa MX100) for further analysis. An insulation box made of bakelite with a low thermal conductivity of 0.233 $Wm^{-1}\,K^{-1}$ is placed beneath the heater to reduce the heat loss. In addition, a total of 4 T-type thermocouples are installed inside the bakelite block at two cross positions to calculate the heat loss from the bottom of the heater. Three independent heaters having identical size (96 mm × 38.5 mm × 1 mm) is placed consecutively below the microchannel heat sink. A schematic showing the heater arrangement is shown in Fig. 3(b). Three autotransformers are used to control power into the heater and the maximum power is 250 W. To minimize the contact resistance amid the heater and the microchannel heat sink, a thermal grease with effective thermal conductivity of 2.8 $W\,m^{-1}\,K^{-1}$ is used, and an additional load cell with supplying load of 100 kgf is also utilized during the experiment. The actual power into the microchannel is calculated as follows:

$$Q_{sup} = P - Q_{loss}. \tag{1}$$

$$Q = \dot{m} c_p (T_{out} - T_{in}). \tag{2}$$

$$Q_{avg} = \frac{Q_{sup} + Q}{2}. \tag{3}$$

where P is the supplied power into the heater and Q_{loss} is the heat floss estimated from the Fourier conduction law of the measured temperatures at the bakelite. Q_{avg} denotes the mathematical average of Q_{sup} and Q. Normally the energy unbalance amid Q_{sup} and Q is less than 5%.

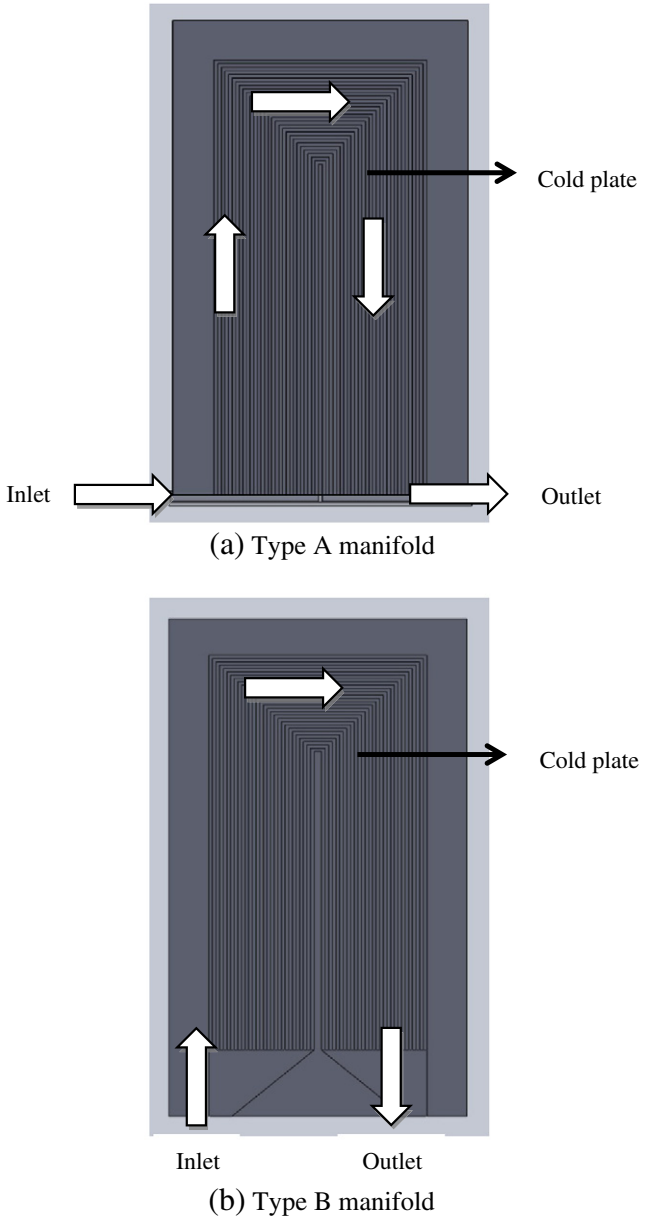

Fig. 2. Schematic of the manifold.

3. Results and discussion

Fig. 4 shows the maximum temperature and the average surface temperature for the test sample for type A manifold subject to inlet temperature. The corresponding inlet temperatures are 25 °C, 30 °C, 35 °C, and 40 °C respectively while the inlet flow rate is 0.71 L/min. In this case, the three independent heat sources are all activated and the total input power, Q_{avg}, is shown in the abscissa. The condition represents the uniform heating situation. As expected, both maximum temperature and average temperature rise with the total input power. On the other hand, the temperature difference between the maximum temperature and average temperature also rises with the supplied power. It is also noted that the maximum temperature is located at the 6th thermocouple location which is near the exit of the cold plate.

Fig. 5 shows the maximum temperature, the average surface temperature, and pressure drops for the type B manifold subject to total input power. The corresponding inlet temperature is 20 °C while the inlet flow rates are 0.46, 0.6, and 0.7 L/min, respectively. As shown in Fig. 5, the pressure drop is reduced with the rise of supplied power. This is because the corresponding viscosity of the water coolant is reduced with the increasing temperature, thereby leading to a slight decline of the pressure drop. The results are analogous to that reported by Toh et al. [3]. It is also noted that the difference between maximum temperature and average temperature for type B manifold is comparatively lower than type A manifold. This is primarily due to the difference of inlet/outlet manifold. The manifold of type B yields a better flow distribution. This is somewhat expected from the inlet configurations where the flow entering the inlet manifold for type A may exhibit a jet flow pattern which may jeopardize the flow distribution. The mal-distribution had been numerically and experimentally verified by Lu and Wang [2], Liu et al. [5], and Wang et al. [9,10]. On the other hand, the inlet configuration of type B manifold had lifted the influence of jet flow, thereby leading to a better flow and temperature distribution. As aforementioned in the Introduction section, the numerical calculation by Lu and Wang [2] also indicated that I type manifold shows the best heat transfer than other arrangements. The present type B manifold is similar to that of I-type arrangement of Lu and Wang [2]. This also substantiates a lower temperature for the type B manifold due to its better heat transfer performance.

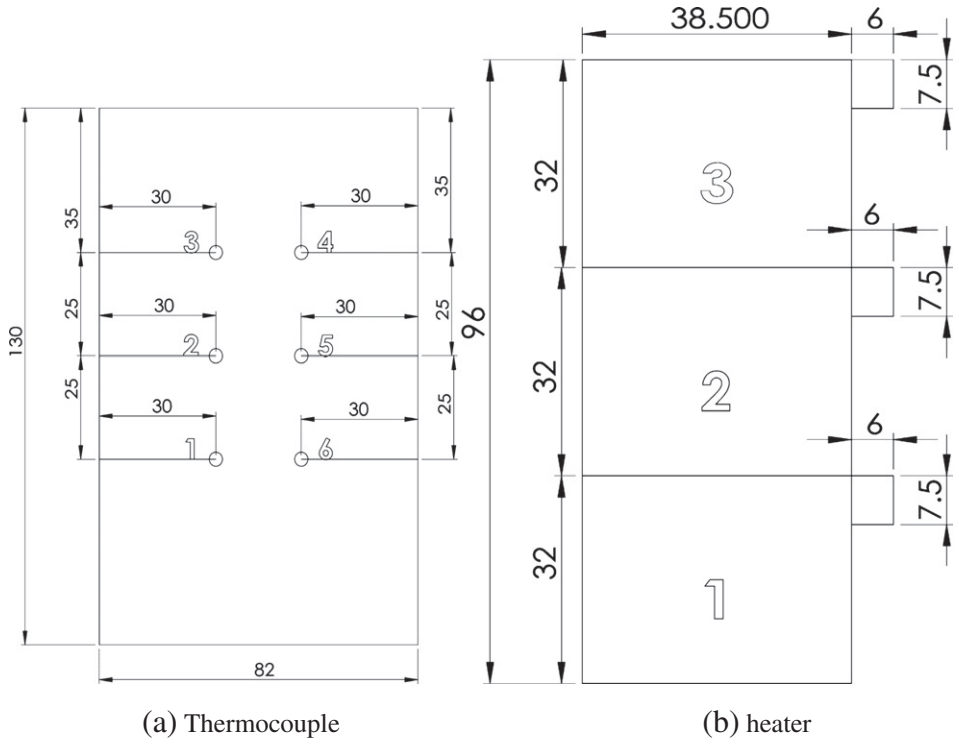

Fig. 3. Schematic of the location of thermocouples and heaters.

The foregoing results are applicable for the uniformly supplied input power, the effect of non-uniform heating subject to various heating locations is shown in Fig. 6(a)–(c). For an easier understanding about the on/off characteristics of the provided heaters, the appeared number in the figure indicates that the corresponding heater is turned on during the test. For the case of two heaters at a specified flow rate, it appeared that the 1–2 heaters show the highest maximum surface temperature, followed by for 1–3 heaters and 2–3 heaters that reveal the lowest temperature. This is especially pronounced at a lower inlet flowrate of 0.46 L/min. Note that the temperature difference amid heaters 1–2 and 2–3 is as high as 10 °C at a total input power of 250 W. The results are quite surprising for both heater size and the total input power are the same. Explanations of this phenomenon are two-fold. Firstly, as is well known, the heat transfer coefficient, or in terms of local Nusselt number Nu, is strongly related to the entrance length. The heat transfer coefficient decreases appreciably from the entrance toward the exit. However, since the present test sample is a 2-pass design where the flow is abruptly forced to turn around at the end of the first pass, thereby the violent flow field and strong mixing occurs that suggests the flow at the beginning of the second pass is similar to that at the first pass. For the 1–2 heater arrangement, the portion of the second pass is at a lower heat transfer performance region (downstream at the second pass).

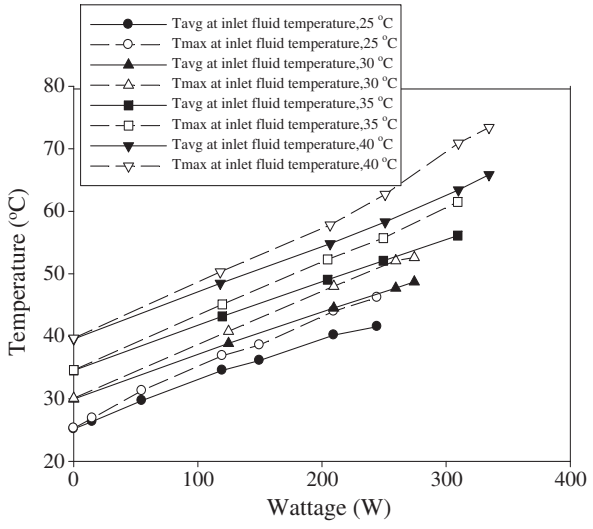

Fig. 4. Variation of maximum and average surface temperature vs. input power subject to various inlet water temperatures.

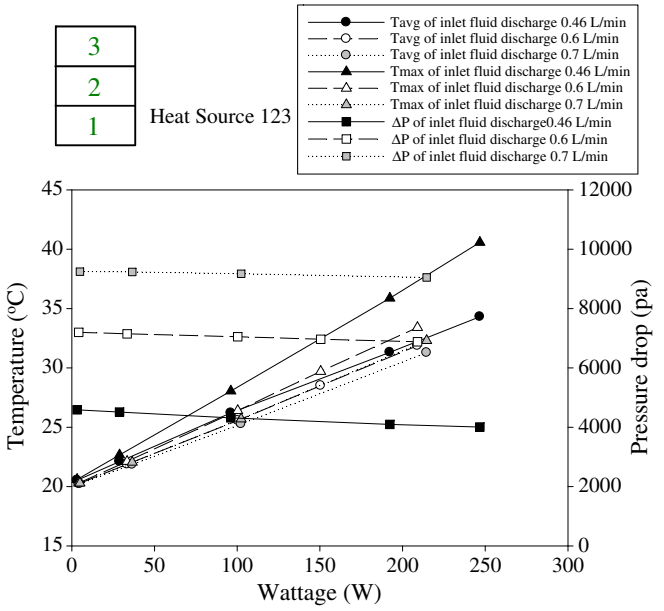

Fig. 5. Variation of maximum temperature, average surface temperature, and pressure drop vs. input power subject to various inlet water flowrates under uniform heating condition.

On the other hand, despite the rear portion of the first pass of the 2–3 heaters region shows a comparatively lower heat transfer performance, it appeared that the portion of the lower heat transfer region is smaller than that of 1–2 arrangements. Secondly, the entrance portion (location of the first heater) which possesses a comparatively lower temperature at the entrance region (heater 1 region) acts as a conduction cooling region for the 2–3 heater arrangement. This provides an additional cooling for the 2–3 heater arrangement. By contrast, the conduction contribution by the location of the third heater subject to 1–2 heater arrangement is appreciably lower since water temperature in this region is much higher than in the entrance region. In summary of the two foregoing reasons, one can see a significant difference of the maximum temperature for the arrangement of the 1–2 heaters and the 2–3 heaters when the inlet flowrate is 0.46 L/min. Note that the performance of the 1–3 heaters falls between 1–2 and 2–3 heaters. This is because its arrangement is between 1–2 and 2–3.

On the other hand, the difference of maximum temperature or average temperature between various heater arrangements (1–3, 1–2, or 2–3) is significantly reduced when the inlet flowrate is raised to 0.6 L/min or 0.7 L/min. Explanation of this result is associated with a much larger increase of pressure drop that leads to a better fluid flow distribution that eventually gives rise to a smaller temperature deviation. In the meantime, a higher flow rate also results in a shorter entrance length. Note that the fully developed length for a flowrate of 0.46 L/min is about 140 mm (based on the evaluation of $x^+_{\text{fully devloped}} = \frac{x}{D_h} R^h ePr \approx 0.04$, Shah and London [11]) but the fully developed length is reduced to 90 mm for an inlet flowrate

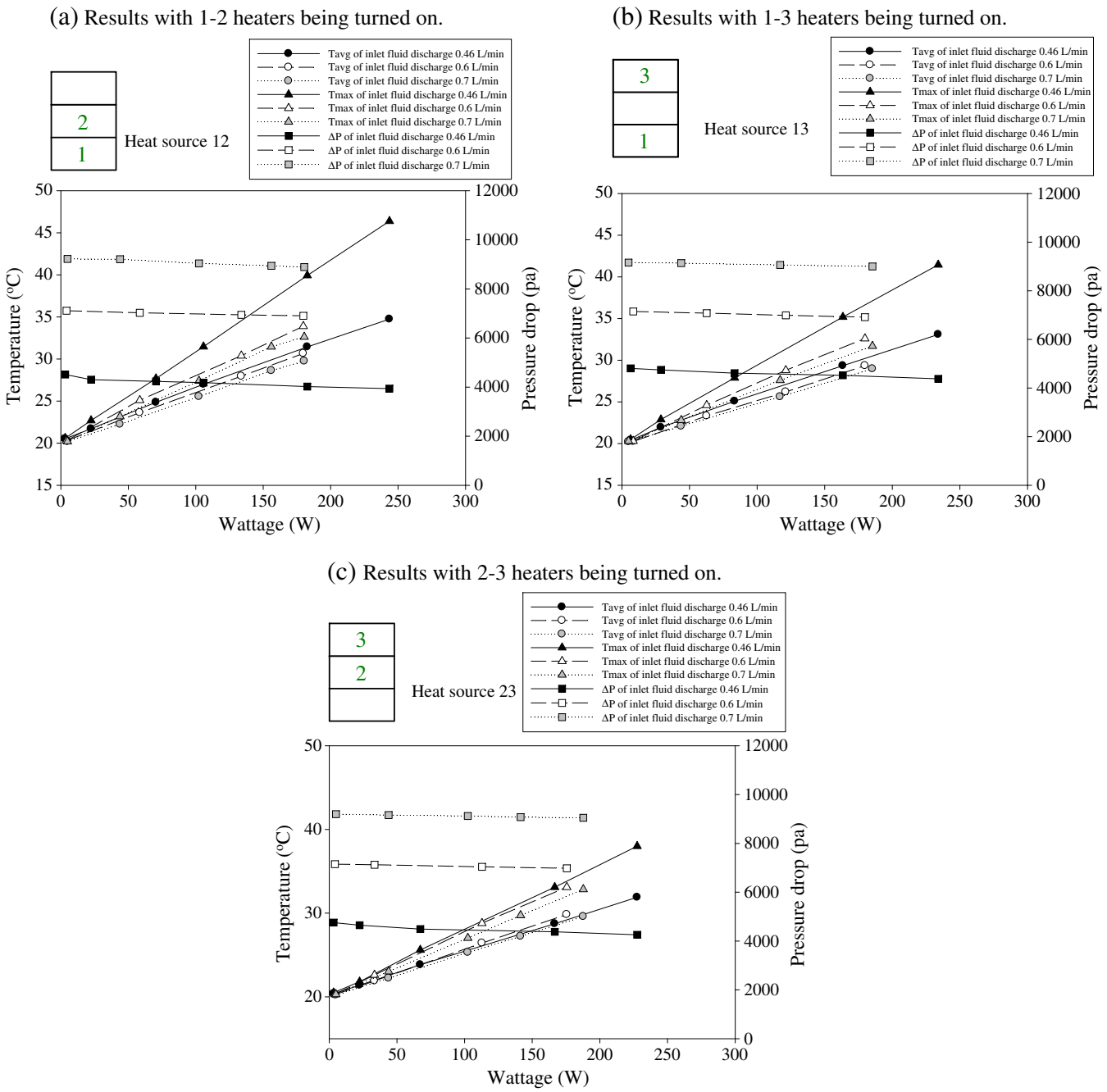

Fig. 6. Variation of maximum temperature, average surface temperature, and pressure drop vs. input power subject to various inlet water flowrates under non-uniform heating condition.

of 0.7 L/min. The results imply that the variation of the heat transfer performance alongside the microchannel heat sink is considerably reduced, and accordingly a less variation of the temperature difference.

4. Conclusions

This study experimentally investigates the performance of microchannel heat sink subject to non-uniform heating. The size of the microchannel heat sink is 132 mm × 82 mm × 6 mm having a two-pass arrangement. Size of the rectangular microchannel is 1 mm × 1 mm and two manifolds are used in this study. The manifolds are characterized as long edge (type A) or short edge (type B). The long edge manifold denotes a side inlet entrance which is normal to the main flow direction while the inlet of the short edge manifold is parallel to the flow direction. Three independent heaters having identical size (96 mm × 38.5 mm × 1 mm) are placed consecutively below the microchannel heat sink. The input power into the heaters can be individually turned on or off to simulate the non-uniform heating condition. Experimental results of this study are summarized in the following:

(1) For either uniform or non-uniform heating condition, both maximum temperature and average temperature rise with the total input power, and this is applicable for both manifolds.
(2) For uniform heating condition, the maximum temperature for type B manifold is much lower than that of type A manifold due to a better flow distribution and heat transfer performance.
(3) The pressure drop is reduced with the rise of supplied power. This is because the corresponding viscosity of the water coolant is reduced with the supplied power, thereby leading to a slight decline of pressure drop.
(4) For non-uniform heating, the maximum temperature and the average temperature depend on the location of heaters. For the same supplied power, it is found that heater being placed at the inlet of the microchannel will give rise to a higher maximum temperature than that being placed at the rear of the heat sink. This phenomenon is especially pronounced when the inlet flowrate is comparatively small and becomes less noted as the inlet flowrate is increased to 0.7 L/min.

Acknowledgments

This work is supported by the National Science Council of Taiwan under contract of 100-2221-E-009-087-MY3. The financial support from the Department of Industrial Technology, Taiwan is also highly appreciated.

References

[1] M.K. Tiwari, I. Zinovik, D. Poulikakos, T. Brunschwiler, B. Michel, 3D integrated water cooling of a composite multilayer stack of chips, Journal of Heat Transfer 132 (2010) 121402-1–121402-9.
[2] M.C. Lu, C.C. Wang, Effect of the inlet location on the performance of parallel-channel cold-plate, Transactions on Components and Packaging Technologies 29 (2006) 30–38.
[3] L.D. Stevanovic, R.A. Beaupre, A.V. Gowda, A.G. Pautsch, S.A. Solovitz, Integral micro-channel liquid cooling for power electronics, integral micro-channel liquid cooling for power electronics, Proceedings of the Applied Power Electronics Conference and Exposition (APEC), Twenty-Fifth Annual IEEE, 2010, pp. 1591–1597.
[4] K.C. Toh, X.Y. Chen, J.C. Chai, Numerical computation of fluid flow and heat transfer in microchannels, International Journal of Heat and Mass Transfer 45 (2002) 5133–5141.
[5] H.S. Park, J. Punch, Friction factor and heat transfer in multiple microchannels with uniform flow distribution, International Journal of Heat and Mass Transfer 51 (2008) 4535–4543.
[6] M.X. Liu, W.J. Sheu, S.B. Chiang, C.C. Wang, PIV investigation of the flow maldistribution in a multi-channel cold plate subject to inlet locations, Journal of Enhanced Heat Transfer 14 (2007) 65–76.
[7] E.S. Cho, J.W. Choi, J.S. Yoon, M.S. Kim, Modeling and simulation on the mass flow distribution in microchannel heat sinks with non-uniform heat flux conditions, International Journal of Heat and Mass Transfer 53 (2010) 1341–1348.
[8] E.S. Cho, J.W. Choi, J.S. Yoon, M.S. Kim, Experimental study on microchannel heat sinks considering mass flow distribution with non-uniform heat flux conditions, International Journal of Heat and Mass Transfer 53 (2010) 2159–2168.
[9] C.C. Wang, K.S. Yang, J.S. Tsai, I.Y. Chen, Liquid flow distribution characteristics in compact parallel flow heat exchangers, part I: typical inlet header, Applied Thermal Engineering 31 (2011) 3226–3234.
[10] C.C. Wang, K.S. Yang, J.S. Tsai, I.Y. Chen, Liquid flow distribution characteristics in compact parallel flow heat exchangers, part II: modified inlet header, Applied Thermal Engineering 31 (2011) 3025–3242.
[11] R.K. Shah, A.L. London, Laminar Flow Forced Convection in Ducts, Academic Press, 1978.